Malaysian Journal of Chemistry, 2020, Vol. 22 (1), 1-7
(Special Issue: *7th International Conference for Young Chemists - ICYC 2019*, Universiti Sains Malaysia)

Effects of Ni_2O_3 Addition on $YBa_2Cu_3O_{7-\delta}(Ni_2O_3)_x$ Superconductor†

A. N. Jannah[1*], I. Mariana[2] and A. Shanthi[1]
[1]*Faculty of Applied Sciences, Universiti Teknologi MARA, Negeri Sembilan Branch, Kuala Pilah Campus, Pekan Parit Tinggi, 72000 Kuala Pilah, Negeri Sembilan, Malaysia*
[2]*School of Applied Physics, Universiti Kebangsaan Malaysia, 43600 Bandar Baru Bangi, Selangor, Malaysia*
*Corresponding author (e-mail: nurjannah@uitm.edu.my)

This study was carried out to investigate the effects of nano nickel oxide (Ni_2O_3) addition on the electrical properties and critical current density (J_c) of $YBa_2Cu_3O_{7-\delta}(Ni_2O_3)_x$ superconductor. The precursor was prepared by the solid state reaction method. The samples were prepared with the prescribed weight percentages of Ni_2O_3 at x = 0, 0.05, 0.10, and 0.15 wt %. The effects of nano Ni_2O_3 were investigated using X-ray diffraction method, scanning electron microscopy, transition temperature, and critical current density (J_c) measurement. The four-point probe technique using the 1 μV/cm criterion was used to measure the critical temperature (T_c) between 50 and 300 K and transport critical current density (J_c) between 30 and 77 K. T_c measurement showed that the critical temperatures of the samples decreased as the composition of Ni_2O_3 increased. The highest J_c was observed in the Ni_2O_3 sample of x = 0.15 wt %. XRD results showed all samples had orthorhombic structure. The grain morphology of every sample was almost similar, except for minor variations in texture and porosity.

Key words: Critical current density; orthorhombic; Ni_2O_3, YBCO

Received: September 2019; Accepted: January 2020

Since the discovery of superconductivity in YBCO at 93 K, the search for a new kind of superconductors has never stopped. The YBCO high temperature superconductor is highly recommended because of its numerous applications (1, 2). It is a layered cuprate superconductor with short coherence length, and the supercurrent could not pass easily through the grain boundary (3). Recent research has reported that nanostructure materials and carbon-based compounds used as high temperature superconductors create high J_c at high magnetic fields (3, 4). Impurity phases and defects present at grain boundaries can act as weak links. Besides, nanoparticle dopants in high temperature superconductors behave as flux pinning centers, which increase the pinning energy (U_j) and critical current density (J_c) (3-11). It is well known that the introduction of artificial pinning centers by the addition or substitution of elements such as micro and nanoparticles, magnetic and non-magnetic materials, and various compounds have successfully improved the properties of $YBa_2Cu_3O_{7-\delta}$ (12-14). In this paper, we report on the study of the influences of Ni_2O_3 on the properties of YBCO high temperature superconductor. The objective of this study is to investigate the effects of Ni_2O_3 addition on the structure and electrical properties of $YBa_2Cu_3O_{7-\delta}$.

EXPERIMENTAL

Materials and Preparation

The $YBa_2Cu_3O_7$ compounds were synthesized by using the solid state reaction method, and all the compounds were ground and powdered using a mortar and pestle for approximately 1 hour into homogenized powder. The chemicals used in this study were yttrium oxide (Y_2O_3), barium carbonate ($BaCO_3$), copper oxide (CuO), and nickel oxide (Ni_2O_3), with high purity (99.9%). Samples were then calcined at 900ºC for 24 hours to remove CO_2. After a slow cooling process in the tube furnace, the calcined powder samples were ground again and a second calcination was performed at 900ºC for 24 hours. Different wt % of mixed powders were pressed into pellets and sintered again at 920ºC for 24 hours in the tube furnace. The transport measurement was carried out using the four-point probe technique, and with the help of liquid helium cryostat to achieve the low temperature. The YBCO samples were examined by T_C measurement to obtain the critical temperature of the samples with Ni_2O_3 (15). The values of the critical current (I_c) were obtained from the I-V measurement and the corresponding values of the critical current density (J_c) were obtained from the maximum current that flowed across the surface area of the samples. X-Ray diffraction was used to determine the structural and phase purity of the superconducting phase of the composite YBCO samples and to indicate phase match by using Bragg's Law formula. Lastly, SEM was used to observe the surface morphology of all the samples and indirectly determine the percentage of elements in the samples by energy-dispersive X-ray spectroscopy (EDX).

†Paper presented at the 7th International Conference for Young Chemists (ICYC 2019), 14-16 August 2019, Universiti Sains Malaysia.

RESULTS AND DISCUSSION

The temperature dependence of the electrical resistivity of the $YBa_2Cu_3O_{7-\delta}(Ni_2O_3)_x$ samples is shown in Figure 1. The temperature at which the value of resistivity drops suddenly, i.e. the appearance of superconducting state occurs, is named as onset critical temperature, $T_{C\ onset}$, and the temperature at which the resistivity of the material becomes zero is called critical temperature, T_C. As shown in Table 1, the T_c values of the $YBa_2Cu_3O_{7-\delta}(Ni_2O_3)_x$ sample systems decreased with the increase of Ni concentration, indicating lower T_c suppression and decrease in carrier concentration with Ni addition. It demonstrates that all of the samples had a linear metallic behavior in the normal state. The study showed that the samples' normal resistivity was reduced by adding Ni_2O_3 to YBCO. Furthermore, it was observed that the transition width (ΔT_c) of the Ni_2O_3-added samples increased with increasing Ni concentration to indicate increased inhomogeneity of the samples. Table 1 also shows the values of critical transition temperatures ($T_{c\text{-}onset}$, T_{c0}) and transition width (ΔT_c) of the Ni_2O_3-added samples. It was found that the non-Ni_2O_3-added sample showed the highest T_c and good superconducting behavior.

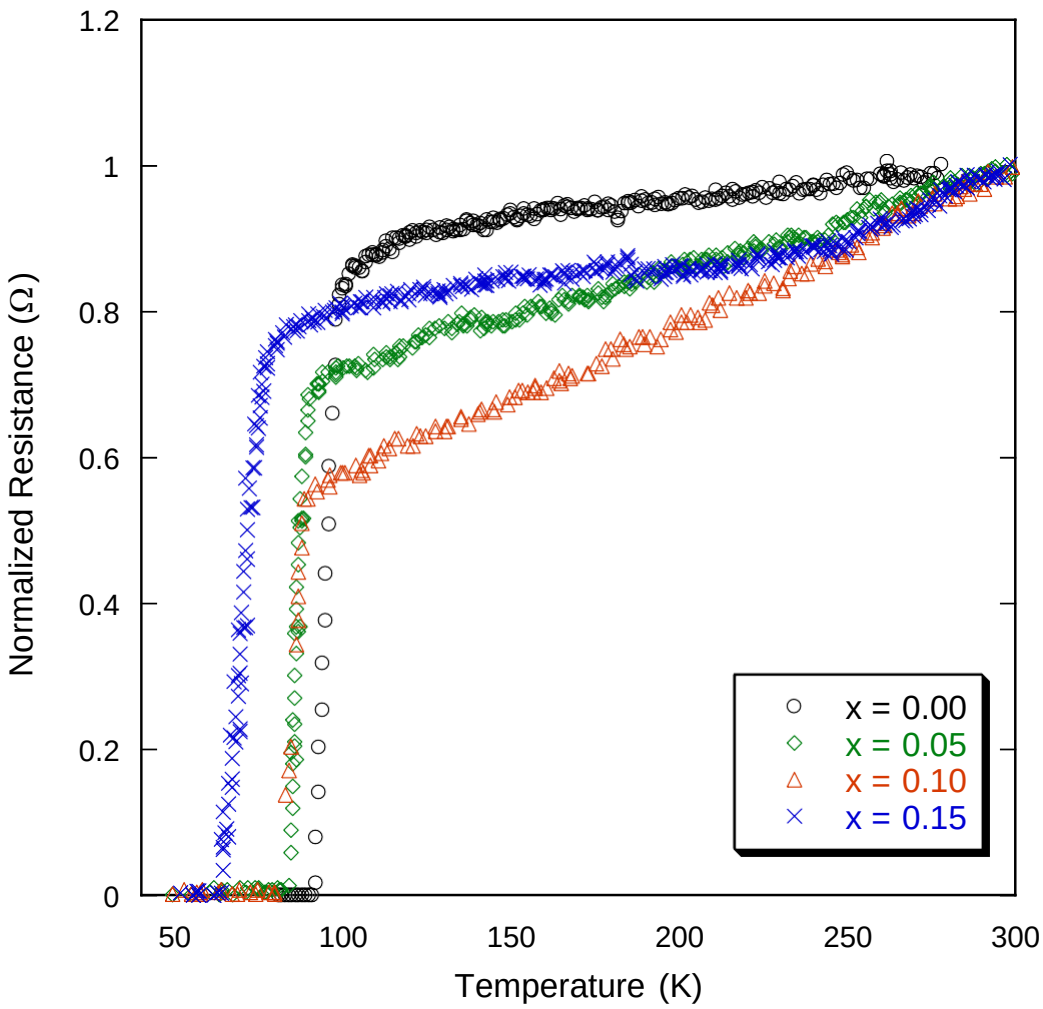

Figure 1. Temperature dependence of resistance for $YBa_2Cu_3O_{7-\delta}(Ni_2O_3)_x$ samples with x = 0.00 – 0.15 wt%

Table 1. $T_{c\text{-}onset}$, $T_{c\text{-}0}$ and ΔT_c for $YBa_2Cu_3O_{7-\delta}(Ni_2O_3)_x$ samples with x = 0.00, 0.05, 0.10, and 0.15 wt %

Composition, x (wt %)	$T_{c\text{-}onset}$ (±1 K)	$T_{c\text{-}0}$(±1 K)	ΔT_c(±1 K)
0.00	98	91	7
0.05	89	80	9
0.10	88	76	12
0.15	76	60	16

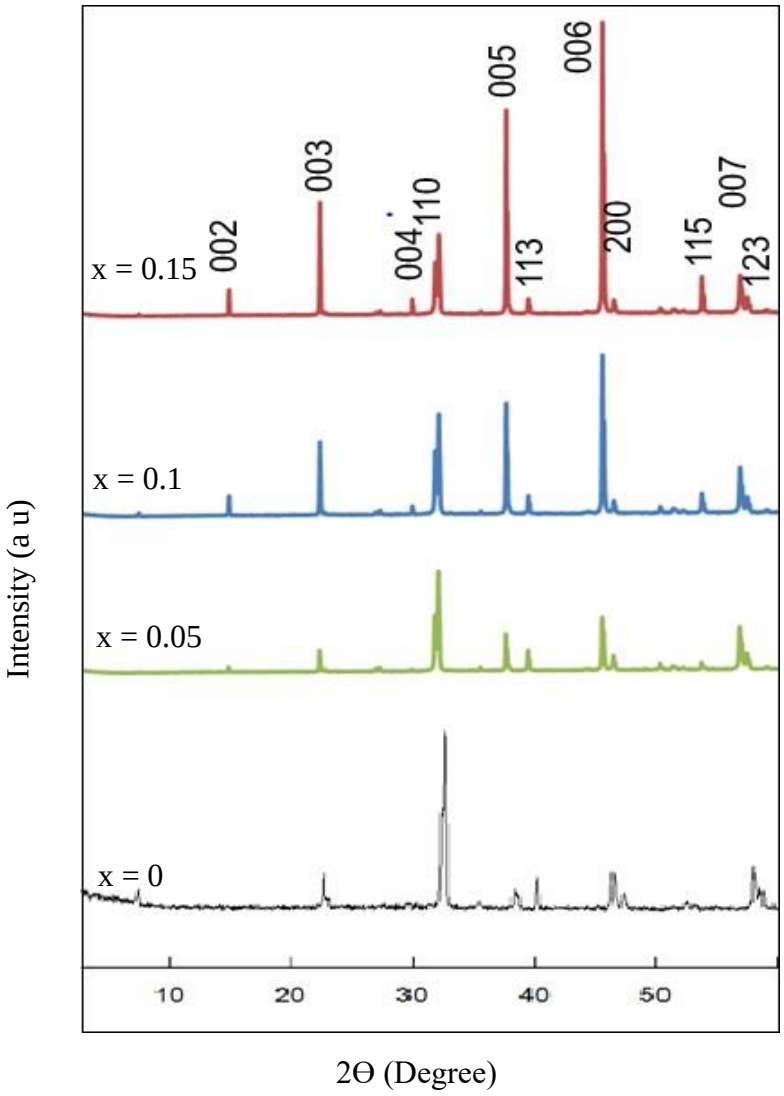

Figure 2. XRD patterns of $YBa_2Cu_3O_{7-\delta}(Ni_2O_3)_x$ samples with x = 0.00, 0.05, 0.10, and 0.15 wt %

Figure 2 shows the XRD results for the samples x = 0 – 0.15 wt % and Y123. Single phase was clearly observed in all samples. All the Ni_2O_3-added samples exhibited orthorhombic structure. With the addition of Ni_2O_3 to the YBCO matrix, no significant variations in lattice parameters were observed. The highest peak was observed at 2θ = 46.540 and peaks indexed at (003), (110), (005), (006) and (007) confirmed the pure phase formation of YBCO superconductor. Hence, the dominance of YBCO phase was clearly observed for all the Ni_2O_3- added samples. However, as Ni_2O_3 was added at different percentages, certain peaks became more intense from x = 0 to 0.15 wt %. The Miller indices were used to determine the lattice parameters (*a*, *b*, *c* parameters). The lattice parameters of the unit cell for all samples are summarized in Table 2. Based on Table 2 and Figure 3, slight changes in lattice parameters *a*, *b* and *c* can be observed. This observation indicates the change of internal lattice strain depends on the addition of Ni in the samples.

Table 2. Lattice parameters of the unit cell

Composition, *x* (wt %)	Lattice parameter (± 0.001 Å)		
	a	*b*	*c*
0.00	3.85800	3.88700	11.71400
0.05	3.82430	3.88850	11.68700
0.10	3.81930	3.88470	11.68340
0.15	3.82260	3.88630	11.66300

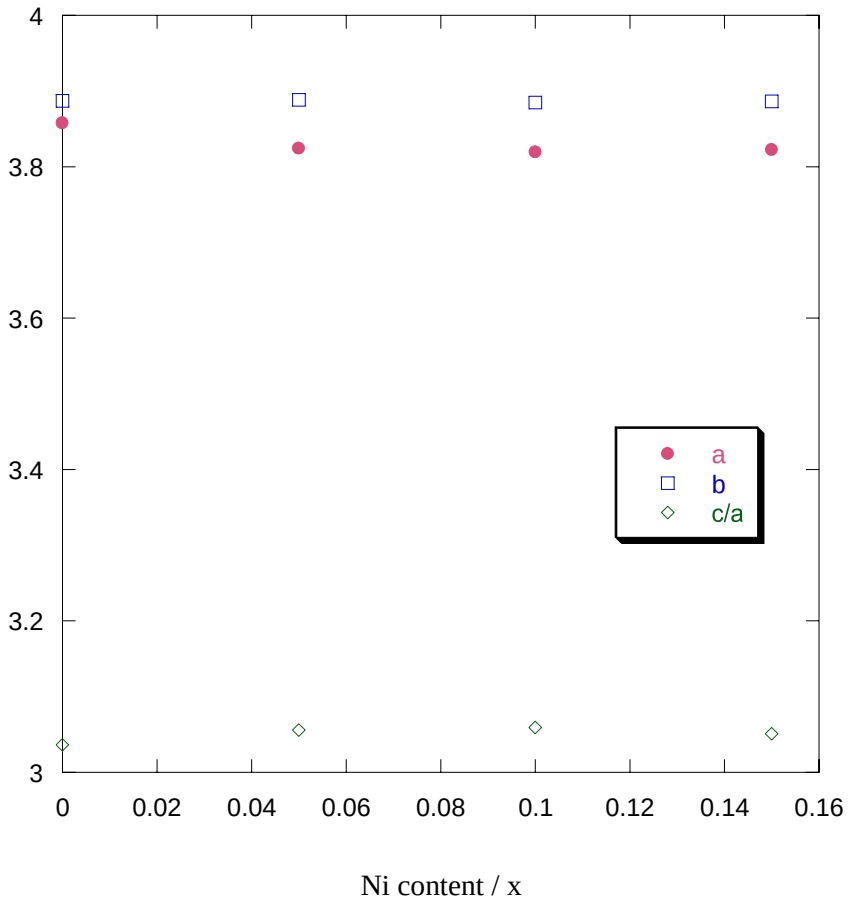

Figure 3. Lattice parameters of $YBa_2Cu_3O_{7-\delta}(Ni_2O_3)_x$ samples with x = 0 - 0.15 wt %

Figure 4 and Table 3 show the variation of J_c with different wt % of Ni_2O_3 doped into the YBCO samples. The J_c values increased with the addition of Ni_2O_3 to the YBCO compounds in a constant magnetic field, but not consistent. The 0.15 wt % of Ni_2O_3 addition sample showed the highest J_c value. We can conclude that Ni_2O_3 addition suppressed the superconductivity but increased the J_c value at certain amounts of addition.

Table 3. Critical current density, J_c for $YBa_2Cu_3O_{7-\delta}(Ni_2O_3)_x$ samples with x = 0.00, 0.05, 0.10, and 0.15 wt % at 30 and 77 K

Composition, x (wt %)	Critical current density, J_c (A/cm^2) **30 K**	**77 K**
0.00	0.15	0.11
0.05	0.36	0.16
0.10	0.39	0.15
0.15	0.42	0.18

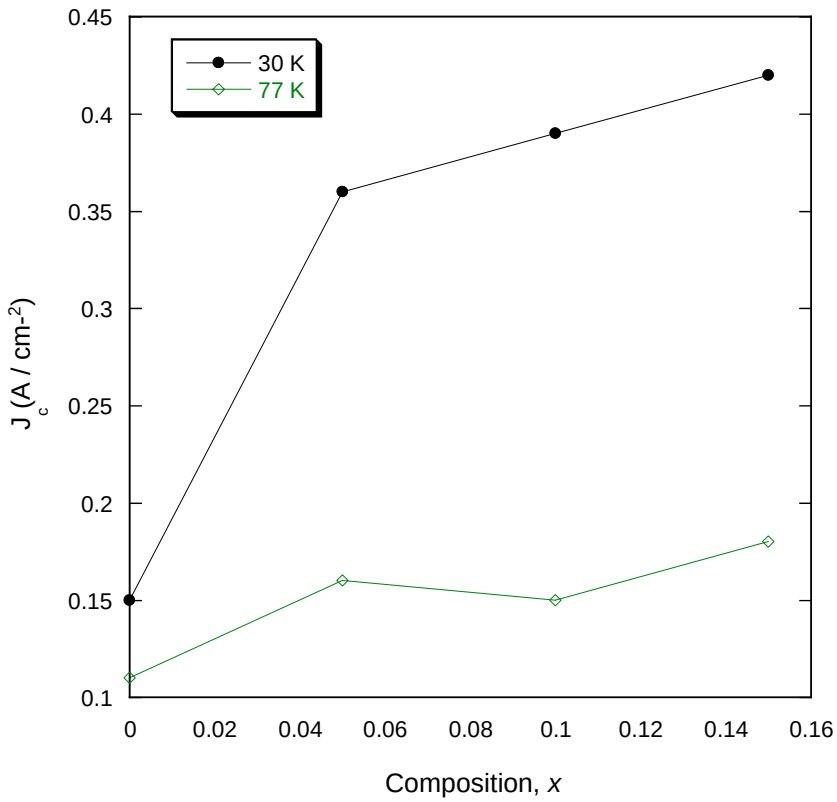

Figure 4. Critical current density, J_c versus Ni_2O_3 content in bulk samples of $YBa_2Cu_3O_{7-\delta}(Ni_2O_3)_x$ at 30 and 77 K

Figures 5(a), (b), (c), and (d) show the surface morphology of the $YBa_2Cu_3O_{7-\delta}$ $(Ni_2O_3)_x$ samples observed using SEM at 1000× magnification. The morphology of the samples could be clearly observed in the SEM images and they revealed no significant change in the grain morphology at lower concentrations. The morphology of all the Ni_2O_3-added samples was almost similar, except for minor variations in texture and porosity. There were pores anticipate between regions of well-connected grains in the non-Ni_2O_3-added sample. The samples with x = 0.15 wt % addition showed compact and densed morphology and this could be a reason for an increase J_c in these samples.

In this study, $YBa_2Cu_3O_{7-\delta}(Ni_2O_3)_x$ (x = 0, 0.05, 0.10, 0.15) were synthesized via the conventional solid state reaction route. By optimizing the ratio of Ni_2O_3 and 123 powders at given amounts, the powders could be uniformly mixed. A methodical study related to the effects of Ni_2O_3 on the transition temperature and microstructure of the samples was performed. All of the samples had a linear metallic behavior in the normal state and transition width, ΔT_c of the Ni_2O_3-added samples increased by increasing Ni concentration. The non-Ni_2O_3-added sample showed the highest T_c and good superconducting behavior. Ni_2O_3 addition has suppressed the superconductivity but increased the J_c value at certain amounts of addition.

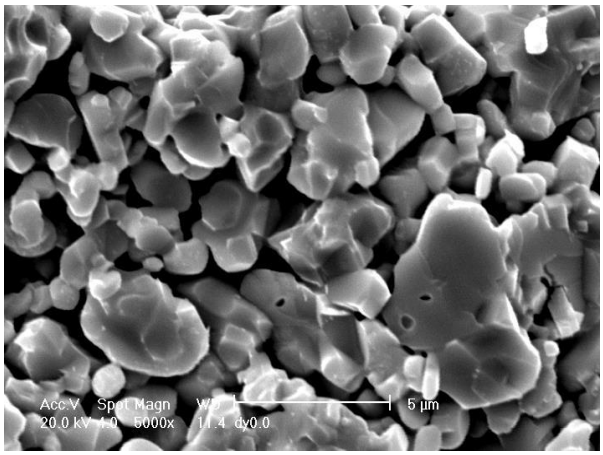

(a)

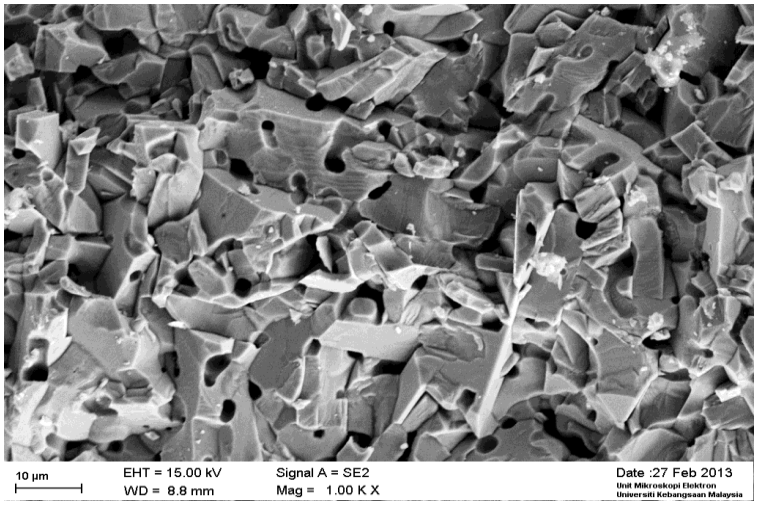

(b)

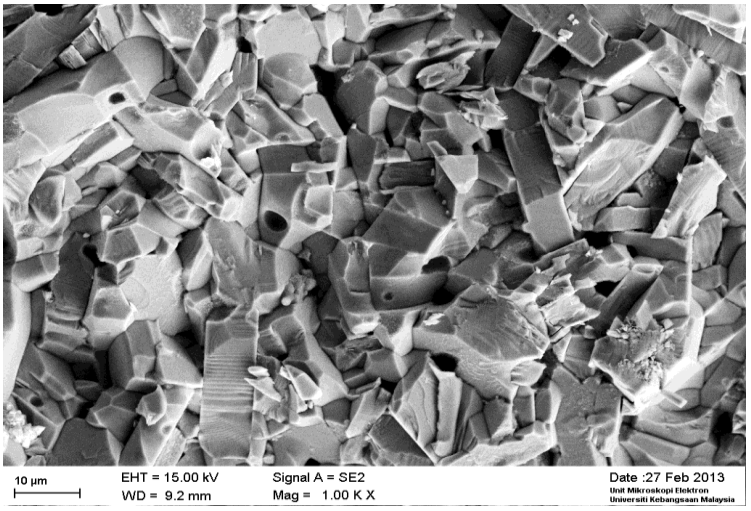

(c)

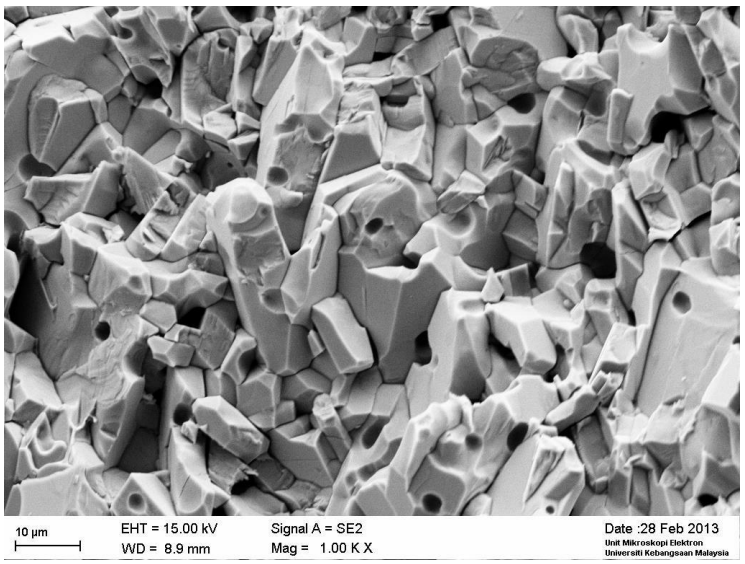

(d)

Figure 5. SEM images for $YBa_2Cu_3O_{7-\delta}(Ni_2O_3)_x$ samples with x = (a) 0.00; (b) 0.05; (c) 0.10; and (d) 0.15 wt %

CONCLUSION

This work showed that Ni_2O_3 addition suppressed the superconductivity but increased the J_c value at certain amounts of addition. Substitution or addition of other elements will be an interesting work for future investigation.

ACKNOWLEDGEMENT

This research was supported by the Ministry of Education, Malaysia, under grant no. FRGS/2/2013/SG02/UKM/01/1 and the Universiti Kebangsaan Malaysia under grant no. UKM-DIP2012-032.

REFERENCES

1. Aghabagheri, S., Rasti, M., Mohammadizadeh, M., Kameli, P., Salamati, H. and Mohammadpour-Aghdam K. (2018) High temperature superconducting YBCO microwave filters, *Physica C: Superconductivity and its Applications*, **549**, 22-26.

2. Mukherjee, P. (2019) Design and development of high temperature superconducting magnetic energy storage for power applications-A review, *Physica C: Superconductivity and its Applications.*

3. Dadras, S., Dehghani, S., Davoudiniya, M. and Falahati, S. (2017) Improving superconducting properties of YBCO high temperature superconductor by Graphene Oxide doping, *Materials Chemistry and Physics*, **193**, 496-500.

4. Dadras, S. and Gharehgazloo, Z. (2016) Effect of Au nano-particles doping on polycrystalline YBCO high temperature superconductor, *Physica B: Condensed Matter*, **492**, 45-49.

5. Vieira, V. N., Pureur, P. and Schaf, J. (2001) The effects of Sr and Ca on the magnetic irreversibility and fluctuation conductivity of YBCO-123, *Physica C: Superconductivity*. **353**, 241-250.

6. Almessiere., M., Slimani, Y., Hannachi, E., Algarni, R. and Azzouz, F. B. (2019) Impact of Dy_2O_3 nanoparticles additions on the properties of porous YBCO ceramics, *Journal of Materials Science: Materials in Electronics*, **30**, 17572-17582.

7. Jannah, A., Abdullah, H., and Abd-Shukor, R. (2015) Enhanced Transport Critical Current Density in Ag-Sheathed $(Bi_{1.6}Pb_{0.4})Sr_2Ca_2Cu_3O_y$ Superconductor Tapes with Different Nano-Sized Co_3O_4 Addition, *Journal of Superconductivity and Novel Magnetism*, **28**, 1471-1476.

8. Tang, T.W., Cao, Y., Wu, D.J. and Xu, K.X. (2016) A modified multi-seeding approach for YBCO bulk superconductors using Y_2BaCuO_5 buffer process, *Journal of Alloys and Compounds*, **673**, 170-174.

9. Ma, Q., Li, X., Ma, Z., Yu, L. and Li, H. (2019) Effect of Nb oping on the microstructure and superconducting properties of FeSe, *Scripta Materialia*, **169**, 65-69.

10. Reigle, A., Mason, K., Slattery, J., Lee, S., Jamison, T., Eggert, A., et. al. (2019) Superconducting properties of In doped ZrNi2Ga1−xInx, *Solid State Communications*, **291**, 28-31.

11. Wang, W., Liu, L., Zheng, T., Liu, S. and Li, Y. (2019) Superconducting properties and microstructures of CeO_2 doped $YBa_2Cu_3O_{7-\delta}$ films fabricated by pulsed laser deposition, *Ceramics International*, **45**, 1998-2002.

12. Nenartaviciene, G., Beganskiene, A., Tautkus, S., Jasaitis, D. and Kareiva, A. (2007) Chromium substitution effects in Y-124 superconductor prepared by aqueous sol–gel method, *Chemical physics*, **332**, 225-231.

13. Sheng, X., Yangni, G. and Xiaoshan, W. (2010) Effects of Yb-doping on flux pinning properties in $YBa_2Cu_3O_{7-\delta}$, *Journal of Rare Earths*, **28**, 431-433.

14. Van Tendeloo, G., Krekels, T., Milat, O. and Amelinckx, S. (1993) Structural effects of element substitution on superconducting properties in 1-2-3 YBCO: an electron microscopy study, *Journal of alloys and compounds*, **195**, 307-314.

15. Schuetze, A. P., Lewis, W., Brown, C. and Geerts, W. J. (2004) A laboratory on the four-point probe technique, *American Journal of Physics*, **72**, 149-153.